Kinetic Modeling of "Living" and Conventional Free Radical Polymerizations of Methyl Methacrylate in Dilute and Gel Regimes

Geoffrey Johnston-Hall and Michael J. Monteiro*

Australian Institute of Bioengineering and Nanotechnology, School of Molecular and Microbial Sciences, University of Queensland, Brisbane QLD 4072, Australia

Received April 30, 2007; Revised Manuscript Received July 6, 2007

ABSTRACT: A universal methodology to obtain the termination rate coefficients in free radical polymerization as a function of conversion and chain length was used to describe the RAFT-mediated "living" radical polymerization (LRP) and conventional free-radical polymerization (FRP) of methyl methacrylate (MMA) up to the glass regime. A composite termination model determined previously using the reversible addition-fragmentation chain transfer−chain length dependent−termination (RAFT-CLD-T) method, based on conversion (x) and chain length (i) dependent termination rate coefficient, $k_t^{i,i}(x)$, data, was the key parameter in obtaining accurate fits to the experimental rate and molecular weight data. Two kinetic modeling approaches were used in this study: (i) model 1: full chain length distributions; (ii) model 2: "method of moments". Both approaches gave excellent agreement with experimental results for the evolution of conversion and MWD for RAFT-mediated polymerizations and accurately described the kinetics after the gel onset conversion. The simulations were also used to validate the accuracy of the RAFT-CLD-T method up to the glass regime to obtain accurate $k_t^{i,i}(x)$ data. Importantly, our simulations gave excellent fits to the rates of polymerization and MWDs for conventional FRP (with broad MWDs), especially the transition from dilute to the gel regime. There is little or no "short−long" termination in RAFT-mediated polymerizations, and therefore the RAFT-CLD-T method provides an ideal approach to probe the mechanism for termination between chains of similar length and their interaction with the polymerizing matrix up to high conversion. We envisage this modeling framework can be easily applied to many other monomers or free radical systems (e.g., ATRP and NMP) and therefore allow highly accurate predictions of polymerization rates and MWDs.

Introduction

The kinetic modeling of conventional free-radical polymerization (FRP) of methyl methacrylate (MMA) has met with limited success due to the difficulty in obtaining accurate rate coefficients for termination, k_t, between two propagating radicals as a function of both conversion, x, and chain length, i. It is now well accepted that bimolecular termination is directly dependent on the mobility of polymeric radicals in the polymerizing medium[1−6] and is therefore influenced by a complex interplay of factors including the diffusion of polymeric radicals, radical chain length,[7] radical size distribution,[8,9] viscosity of the medium, and polymer concentration.[2] This dependence is exacerbated when the polymerization undergoes autoacceleration, a phenomenon known as the gel (or Trommsdorf) effect, and is exhibited by the rapid increase in the rate of polymerization due to a decrease in k_t. Methods for obtaining k_t have commonly proven to be the major hurdle in deriving accurate kinetic models, especially as the polymerization goes from the dilute through to the gel regime.

Recently, a number of methods based on pulsed laser polymerization (PLP)[10] and "living" radical polymerization (LRP)[11−13] have been used to determine accurate values of k_t and have led to a significant advance in describing termination between polymeric radicals of the same chain length, i (i.e., $k_t^{i,i}$). One model-independent method, based on reversible addition-fragmentation chain transfer (RAFT)—known as the RAFT chain length dependent termination or RAFT-CLD-T method[11]—allows the evaluation of $k_t^{i,i}$ over a range of chain lengths and conversions (x) from a single experiment. The RAFT-CLD-T method has since been used to study $k_t^{i,i}$ for methyl methacrylate,[14,15] vinyl acetate,[16] and various acrylates.[17−20] Importantly, this method has now also been applied to simultaneously evaluate the effect of polymer concentration and chain length on k_t,[15,16,20] since chain length increases linearly with conversion in LRP.[21,22]

The chain length dependence of termination is typically described according to a simple power law expression[23]

$$k_t^{i,i} \propto k_t^{1,1} i^{-\alpha} \tag{1}$$

where the power law exponent, α, represents the dependence on chain length. The main advantage of using the RAFT-CLD-T method is that at any given conversion (or time) the radical chain length distribution is close to a Poisson distribution (i.e., a very narrow molecular weight distribution, MWD).[24] Hence, for the termination between two radicals of length i and j, it can be assumed that i and j are approximately equal.

Recently, we studied[15] the chain length and conversion dependent termination rate coefficient, $k_t^{i,i}(x)$, profile of MMA using the RAFT-CLD-T method. At low conversions we found that $k_t^{i,i}(x)$ could be described according to two regimes: a "short" chain length regime (for $i < 100$) with an α of 0.65 and a "long" chain length regime with an α of 0.15. At intermediate and high conversions, beyond the gel effect, we found that the chain length dependence scaled according to $\alpha_{gel} = 1.8x + 0.056$ for any i. Importantly, we showed that the transition between the dilute solution and gel regimes (i.e., the onset of the gel effect) closely correlated with the theoretical polymer overlap concentration, c^*. From these dependencies we were able to construct a chain length dependent composite

* To whom correspondence should be addressed: e-mail m.monteiro@uq.edu.au.

10.1021/ma070984d CCC: $37.00
Published on Web 08/29/2007

k_t model that allowed the prediction of $k_t^{i,i}(x)$ up to the glass region. Our model even predicted the smooth transition between the dilute and gel regime, which was commonly represented as a sharp transformation.[15]

The aim of this work is to use the composite k_t model derived from our previous work[15] in a kinetic model to describe both RAFT-mediated and conventional free-radical polymerizations over a range of experimental conditions to accurately predict and fit experimental rates of polymerization and MWD data. In particular, experiments were carried out under conditions in which autoacceleration in polymerization rate was observed in the conversion profiles. Modeling has proven to be an invaluable tool for understanding the RAFT process, providing opportunities to control reaction rates,[25] molecular weights,[25] block copolymer structure,[26,27] and even molecular weight distributions.[26,28] However, these models could be significantly improved with the accurate expression for $k_t^{i,i}(x)$ as a function of both x and i and can allow LRP experiments to be designed to produce polymer with minimal dead polymer[26]—a significant advance for making novel architectures (e.g., stars,[29] and polymeric dendrimers[30]). The ultimate test of our composite k_t model is its incorporation in a kinetic model to fit not only with "living" radical polymerizations but also conventional free-radical polymerizations, especially when the polymerization goes from dilute solution into the gel regime. We will carry out an in-depth analysis of the RAFT-CLD-T method in both the dilute solution and gel regimes and validate the assumption that $\langle k_t \rangle$ at each conversion (and therefore i) is approximately equal to $k_t^{i,i}(x)$ due to the narrow MWD found in "living" radical polymerizations. This work will also address the contribution and importance of "short−long" termination in conventional FRP and RAFT-mediated "living" radical polymerizations.

Scheme 1. Simplified RAFT Mechanism Based on Degenerative Chain Transfer[a]

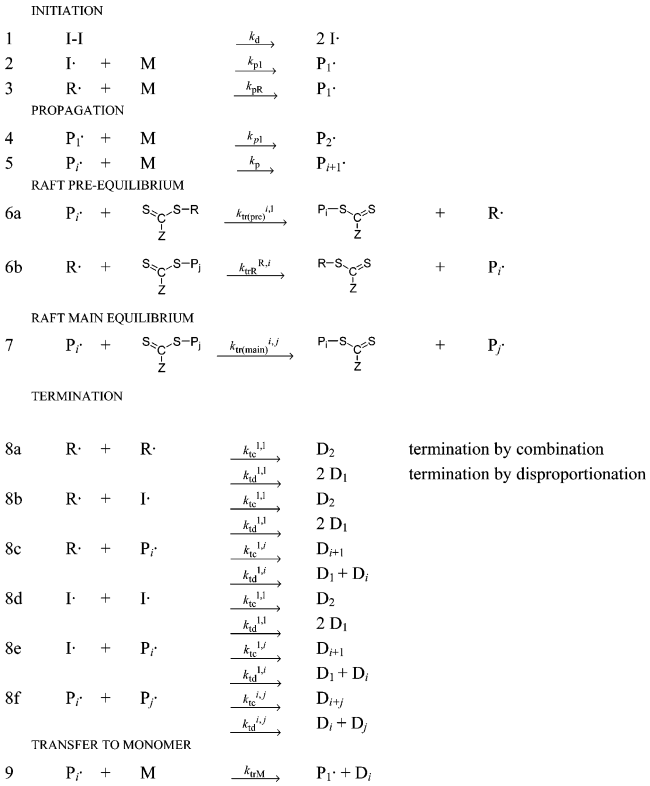

[a] The notations used in the scheme are as follows: I−I = initiator (e.g., AIBN), M = monomer, P_i = polymeric radical of i monomer units, and D_i = dead polymer of i monomer units.

Experimental Section

Chemicals. Methyl methacrylate (MMA, 99%, Aldrich) was purified by passing through a basic alumina column (70−230 mesh) to remove inhibitors prior to use. 2,2-Azobis(isobutyronitrile) (AIBN, 99%, DuPont) was purified by recrystallization from methanol. 2-Cyanoprop-2-yl dithiobenzoate (CPDB) was prepared according to the literature procedure.[14]

Typical RAFT Polymerization. MMA monomer (2 mL, 9.34 mol/L), AIBN (0.000 67 g, 2.01 mmol/L), and CPDB (0.004 40 g, 9.93 mmol/L) were transferred to a reaction vessel, degassed by four successive freeze−pump−thaw cycles, and polymerized at 80 °C. Conversion was measured gravimetrically by drying the samples in a vacuum oven at ambient temperature until at constant weight, and the molecular weight distribution was determined by size exclusion chromatography (SEC). The polymerization data were taken from work previously published.[15]

Typical Free-Radical Polymerization (FRP). MMA monomer (2 mL, 9.34 mol/L) and AIBN (0.00067 g, 2.01 mmol/L) were transferred to a reaction vessel, degassed by four successive freeze−pump−thaw cycles, and polymerized at 80 °C. Conversion was measured gravimetrically by drying the samples in a vacuum oven at ambient temperature until at constant weight, and the molecular weight distribution was determined by SEC.

Typical Differential Scanning Calorimetry (DSC) RAFT Polymerization of MMA. Differential scanning calorimetry (DSC) polymerizations were all performed in duplicate. MMA monomer (2 mL, 9.34 mol/L), AIBN (0.000 67 g, 2.01 mmol/L), and CPDB (0.004 40 g, 9.93 mmol/L) were transferred to a reaction vessel, degassed by four successive freeze−pump−thaw cycles, and placed under nitrogen in a glovebag. DSC samples were prepared by pipetting the solution into gastight DSC pans and recording sample weight by mass difference. The sample weights in the DSC pans ranged between 30 and 60 mg. The polymerizations were carried out isothermally at 80 °C, and the heat of polymerization was measured by comparing the heat flow from the polymerization pan and an empty pan on a Perkin-Elmer DSC 7 with a TAC 7/DX Thermal Analysis Instrument Controller. The DSC instrument was calibrated with a standard indium sample of known mass, melting point temperature, and associated enthalpy change. The rate of polymerization, R_p, and monomer conversions, x, were calculated using literature values for the heat of polymerization of MMA ($\Delta H_p = -52.8$ kJ mol^{-1}).[31]

Size Exclusion Chromatography (SEC). Size exclusion chromatography (SEC) measurements were performed using a Waters Alliance 2690 separations module equipped with an autosampler, column heater, differential refractive index detector, and a photodiode array (PDA) connected in series. HPLC grade tetrahydrofuran was used as eluent at a flow rate of 1 mL min^{-1}. The columns consisted of three 7.8 × 300 mm Waters Styragel GPC columns connected in series, comprising two linear Ultrastyragel and one Styragel HR3 columns. Poly(methyl methacrylate) (PMMA) standards ranging from 2 000 000 to 540 g mol^{-1} were used for calibration.

Computer Simulations. All kinetic simulations were performed by solving differential equations using a program written for the software package MATLAB (version 7.1) on an IBM compatible 2.8 GHz, 3 GB RAM, Intel Xeon processor. The differential equations based on Scheme 1 can be found in the Supporting Information and were solved using a multistep numerical variable order method. The kinetic parameters used for all simulations are listed in Table 1, unless otherwise stated.

Model Development

The complex addition-fragmentation steps for RAFT were simplified to the degenerative chain transfer model (Scheme 1). This procedure was used as it is computationally less demanding than solving for all addition-fragmentation steps and

Table 1. Kinetic Parameters Used in the Simulations to Model the RAFT-Mediated Bulk Polymerization of Methyl Methacrylate (MMA) in the Absence and Presence of RAFT Agent, Cyanoisoprop-2-yl Dithiobenzoate (CPDB), and Initiated with Azobis(isobutyronitrile) (AIBN) at 80 °C

parameter	value	ref
k_p/L mol^{-1} s^{-1}	1332	58
k_{tc}/k_{td}	0.01	59
k_d	1.1×10^{-4}	17
f	0.7	60
k_{pR} / L mol^{-1} s^{-1}	$10k_p$	
$C^0_{tr(main)}$	140	61
$C^0_{tr(pre)}$	15.2	14
C^0_{trR}	0[a]	
$k^0_{tr(pre)}$/ L mol^{-1} s^{-1}	$C^0_{tr(pre)}k_p$	
$k^0_{tr(main)}$/L mol^{-1} s^{-1}	$C^0_{tr(main)}k_p$	
k^0_{trR}/L mol^{-1} s^{-1}	$C^0_{trR}k_p$	
k_{trM}/L mol^{-1} s^{-1}	0.024	62
$[MMA]_0$/mol L^{-1}	9.34	
$[RAFT]_0$/mol L^{-1}	0.05[a]	
$[AIBN]_0$/mol L^{-1}	0.01[a]	
T/°C	80	

[a] Unless defined otherwise.

Table 2. Kinetic Parameters Used To Model the Conversion and Chain Length Dependent Termination Rate Coefficient, $k_t^{i,i}(x)$, of Methyl Methacrylate (MMA) at 80 °C

parameter	value	ref
$k_t^{1,1}$	1.2×10^9	14
α_S	0.65	14
i_{SL}	100	14
α_L	0.15	14
i_{gel}	$[(x/2.628)^{-1/0.21}]/mw$	15
α_{gel}	$1.8x + 0.056$	15

is accurate provided that fragmentation of the intermediate radical is fast and side reactions, such as slow fragmentation (SF)[32] or intermediate radical termination (IRT),[25a,b] as well as impurities[25c] are negligible. We have shown this to give reliable data.[27]

The model required other parameters: chain length and conversion dependent termination (step 8 in Scheme 1), chain length dependent propagation, and chain length and conversion dependent addition of polymeric radicals to dormant RAFT species (steps 6 and 7 in Scheme 1). Two approaches were used to simulate the "living" radical and conventional free-radical polymerization of MMA: (1) solving the differential equation over the full distribution of chain lengths, which is computationally expensive and could only be used for polymerizations where the radical, dormant, and dead chains are small (e.g., ranging between 1 and 1600 monomer units), and (2) solving the kinetic steps using the method of moments[33] and calculating the chain length dependent rate coefficients by incorporating either a Poisson distribution for radical, dormant, and dead species in RAFT-mediated polymerizations or a Schulz−Flory distribution function[34] for radical and dead species in conventional FRPs. Practices such as this, as well as "coarse graining",[35] are commonly used to simplify the calculations associated with modeling full chain length distributions. The use of the Schulz−Flory distributions in predicting chain length distributions in conventional FRP is a well-used procedure.[36]

Below is a description of how the various chain length dependent parameters were incorporated into the simulations. It should be noted that our model used known rate coefficients from literature, and importantly parameter fitting was not used in the simulations.

Chain Length Dependent Termination (Composite Model). Conversion and chain length dependent termination rate coefficients, $k_t^{i,i}(x)$, were introduced into the simulations using the composite model described by eqs 2−5. Readers are directed to ref 15 for a comprehensive description and derivation of these expressions.

For $i < i_{gel}$:

$$k_t^{i,i} = k_t^{1,1} i_x^{-\alpha_S} \qquad \text{for } i_x < i_{SL} \tag{2}$$

$$k_t^{i,i} = k_t^{1,1} i_{SL}^{(\alpha_L-\alpha_S)} i_x^{-\alpha_L} \qquad \text{for } i_x \geq i_{SL} \tag{3}$$

For $i \geq i_{gel}$:

$$k_t^{i,i} = k_t^{1,1} i_{gel}^{(\alpha_{gel}-\alpha_S)} i_x^{-\alpha_{gel}} \qquad \text{for } i_x < i_{SL} \tag{4}$$

$$k_t^{i,i} = k_t^{1,1} i_{SL}^{(\alpha_L-\alpha_S)} i_{gel}^{(\alpha_{gel}-\alpha_L)} i_x^{-\alpha_{gel}} \qquad \text{for } i_x \geq i_{SL} \tag{5}$$

where $k_t^{1,1}$ represents the termination rate coefficient for two 1-mers found from the intercept of the slope in the dilute and "short" chain length regime (for $i < 100$, $\alpha = 0.65$), α_S is the power law dependent exponent for "short" chains in dilute solution, α_L is the power law exponent for "long" chains in dilute solution, i_{SL} is the dilute solution "crossover" chain length when power laws for termination change from "short" chains to "long" chains, and α_{gel} is the power law exponent for termination in the gel regime. Values for all these parameters are given in Table 2. One of the most important parameters is i_{gel}, the characteristic chain length at onset of the gel effect determined from the RAFT-mediated polymerization,[15] and is used as a main criterion to determine $k_t^{i,i}$ irrespective of the conversion. Should a chain be greater than i_{gel} in the dilute regime, the model considers it to behave as a slow diffusing chain in the gel regime, which becomes important in conventional FRP where the radical distribution is broad.

Previously, we showed that eqs 2−5 were able to fit experimental $k_t^{i,i}(x)$ data found over a range of CPDB concentrations for RAFT-mediated polymerizations of MMA. Three distinct $k_t^{i,i}(x)$ regimes were observed and accounted for in the model: two in the dilute regime, in which the first corresponded to "short" radical termination and scaled with $\alpha_S = 0.65$ and the second corresponded to "long" chain radical termination and scaled with $\alpha_L = 0.15$. The third regime was the gel regime and scaled according to $\alpha_{gel}(x) = 1.8x + 0.056$. The onset of this third regime was found to correlate closely with the polymer−polymer overlap concentration (c^*).[15]

Chain Length Dependent Propagation. It has been found that the propagation rate coefficient (k_p) is chain length dependent for the addition of the first 10 monomer units, after which k_p becomes relatively constant.[37−40] It has been theoretically predicted that k_p is ∼10 times greater for a 1-mer than the "long" chain average k_p. In the simulations, the propagation rate coefficients for initiator fragments, leaving group radicals, and 1-mers (k_{p1} and k_{pR}, Scheme 1) were all set to $10k_p$.

Determination of k_{tr} for Propagating Radicals, *i*, to Dormant Species, *j* ($k_{tr}^{i,j}$). The rate coefficients of transfer in the preequilibria and main equilibria, $k_{tr(pre)}^{i,1}$ and $k_{tr(main)}^{i,j}$, were calculated according to the following expressions (see Supporting Information for the derivation of eqs 6 and 7):

$$k_{tr(pre)}^{i,1} = \frac{k_{add}^{i,1}}{2} \tag{6}$$

$$k_{tr(main)}^{i,j} = \frac{k_{add}^{i,j}}{2} \tag{7}$$

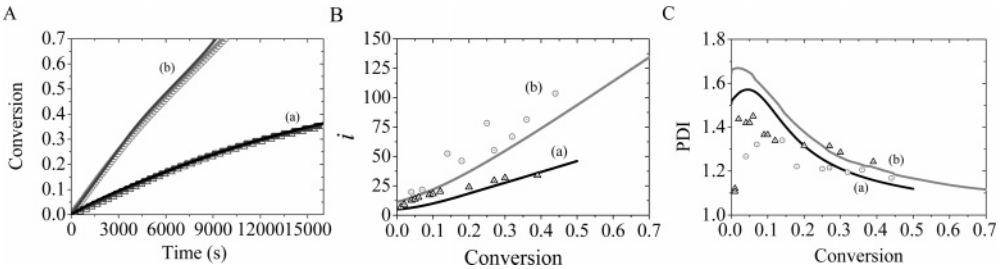

Figure 1. Kinetic plots for the RAFT-mediated bulk polymerization of methyl methacrylate (MMA, 9.34 M) in the presence of 2-cyanoprop-2-yl dithiobenzoate (CPDB), and initiated with azobis(isobutyronitrile) (AIBN) at 80 °C. Curves correspond to (a) [CPDB] = 100 mM and [AIBN] = 2.54 mM (Δ) and (b) [CPDB] = 54 mM and [AIBN] = 8.8 mM (○). Solid lines are simulated kinetic plots of the full molecular weight distribution using the following kinetic parameters: $C^0_{tr(pre)} = 15.2$,[14] $C^0_{tr(main)} = 140$,[61] $k_p = 1330$ L mol^{-1} s^{-1}, $f = 0.7$, and $k_d = 1 \times 10^{-4}$ s^{-1}.

Chain Length Dependent Rate Coefficient for Radical Addition to Dormant Species. The addition coefficient between radical species, *i*, and dormant species, *j*, are analogous to the bimolecular termination reaction between two propagating radicals *i* and *j*. The chain length dependent addition rate coefficient, $k^{i,j}_{add}$, was therefore implemented into the simulations using the encounter pair model and the conversion and chain length dependent $k^{i,j}_t$ according to

$$k^{i,j}_{add} = \left(\frac{1}{k^0_{add}} + \frac{1}{k^0_t} + \frac{1}{k^{i,j}_t}\right)^{-1} \quad (8)$$

Hence, eq 8 is calculated from eqs 2−5 (see Supporting Information for the derivation of eq 8) and by assuming $k^0_{add} = C^0_{tr(main)}k_p$ and $k^0_t = k^{1,1}_t$ (see Table 1).

Mean Approximation. In most modeling procedures, $k^{i,j}_t$ is calculated from the mean of $k^{i,i}_t$ and $k^{j,j}_t$. Conventionally, the diffusion mean (DM), geometric mean (GM), and harmonic mean (HM) approximations have been used to estimate $k^{i,j}_t$. However, there is no one universally accepted approach. In fact, the nonphysical GM (eq 9) has been widely used and gained much support in the literature.[41−43] Simulations using the DM, GM, and HM models (results not shown here) showed that the GM gave the best agreement with experiment, particularly at intermediate and high conversions. Thus, the GM was used in all subsequent simulations.

$$k^{i,j}_t = (k^{i,i}_t k^{j,j}_t)^{1/2} \quad \text{(GM)} \quad (9)$$

Modeling Radical Chain Length Distributions in RAFT. Model 1: Full Chain Length Distribution. Chain length dependent termination dictates that the average experimentally observable termination rate coefficient, $\langle k_t \rangle$, is a weighted average of all the individual termination rate coefficients, $k^{i,j}_t$. Thus, at any point in time the average observable $\langle k_t \rangle$ is a function of all the individual termination events according to eq 10.[8] Simulations were therefore performed by solving differential equations for all values of *i* and *j* (see Supporting Information) for RAFT polymerizations involving high concentrations of RAFT agent (e.g., 54 and 100 mM CPDB).

$$\langle k_t \rangle = \frac{\sum_{i=1}^{\infty}\sum_{j=1}^{\infty} k^{i,j}_t [P^\bullet_i][P^\bullet_j]}{\left(\sum_{i=1}^{\infty}[P^\bullet_i]\right)^2} \quad (10)$$

Model 2: Method of Moments−Using Poisson and Schulz−Flory Functions for the Radical Distribution. When modeling the polymerization kinetics with low concentrations of CPDB (e.g., 5, 10, and 20 mM), the full chain length distribution strategy (model 1) was computationally demanding due to the very large number of differential equations required to be solved. Hence, in order to carry out these simulations for RAFT-mediated polymerizations (with low PDIs), the method of moments, approximating a Poisson distribution function for the radical chain length distribution (by solving eq 2) and using our chain length and conversion dependent composite termination model (see above) strategy, was used to determine values of $k^{i,j}_t$. Comparisons between models 1 and 2 at the high CPDB concentrations were in excellent agreement, suggesting our strategy (model 2) provides an accurate description of the polymerization kinetics. Therefore, the same methodology was used for conventional free-radical polymerizations, but a Schulz−Flory radical distribution function[34] was used to determine the radical distribution.

Results and Discussion

Model 1: Full Chain Length Distribution. RAFT Polymerization with High Concentrations of CPDB. Simulations using model 1 were performed by solving differential equations for chains of all lengths between 1 and 1600 monomer units. This approach is the most accurate way to simulate the polymerization kinetics but is limited to small chains (up to 1600 monomer units) and narrow MWDs. Figure 1 shows the fit between experiment and simulation using model 1 for the bulk polymerizations of MMA at the two highest CPDB concentrations (54 and 100 mM) and initiated with AIBN at 80 °C. There is excellent agreement between the simulations and experiments for the conversion vs time profiles (Figure 1A). The simulations could also accurately predict the number-average chain length (*i*) and polydispersity (PDI) as a function of conversion (Figure 1B,C). The results suggest that model 1, the composite $\langle k_t \rangle$ model, and the parameters used above provide an accurate kinetic description of RAFT-mediated polymerizations.

Accuracy of the RAFT-CLD-T Method to Determine $k^{i,i}_t(x)$. As discussed earlier, it is assumed that the averaging of all termination events in RAFT-based polymerizations results in $\langle k_t \rangle$ being approximately equal to $k^{i,i}_t(x)$. The excellent fit between simulation and experiment in Figure 1 supports this postulate. However, in any RAFT polymerization there are always small radicals generated from initiator (AIBN) over the course of the polymerizations. This may suggest that termination is not dominated by *i*−*i* termination events alone but may also include an appreciable amount of *i*−*k* termination (where *k* could be small and less than 10 units).

On the basis of the excellent fit of simulations using model 1 with experiment, we used the chain length radical distribution obtained from simulations at each conversion (Figure 2) to

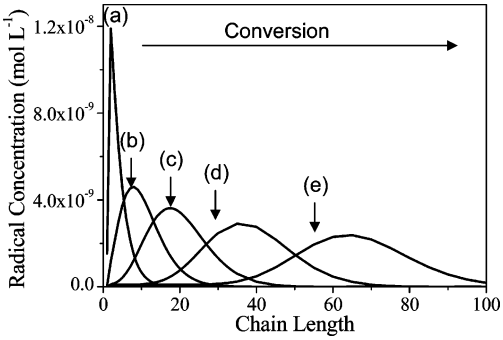

Figure 2. Effect of conversion on the radical chain length distribution (CLD) predicted by model 1 (based on the full chain length distribution) for a RAFT-mediated bulk polymerization of methyl methacrylate (MMA, 9.34 M) in the presence of RAFT agent (CPDB, 50 mM) initiated with azobis(isobutyronitrile) (AIBN, 10 mM) at 80 °C. Chain length distributions are shown for (a) 1% conversion, (b) 5% conversion, (c) 10% conversion, (d) 25% conversion, and (e) 45% conversion.

calculate the rate of termination only between chains of length i (R_t^i), where i is defined as the number-average chain length. The radical distributions in Figure 2 broadened with conversion even though the PDIs were low and similar for all distributions. Hence, the question remains as to the influence of $i-i$ termination and whether the assumption that $\langle k_t \rangle$ is equal to $k_t^{i,i}(x)$ up to high conversions is valid in RAFT-mediated polymerizations?

The overall rate of termination (R_t) for the full radical distribution can be calculated using eq 11, and therefore the contribution of $i-i$ termination to the overall rate of termination can be assessed from the ratio of R_t^i/R_t. Figure 3 clearly shows for a typical RAFT-mediated polymerization of MMA in the presence of CPDB and AIBN that the ratio of R_t^i/R_t (at $\mu = 0$, where μ is defined as the deviation of monomer units from i) was close to zero over the full conversion range, suggesting that $i-i$ termination is negligible compared to the sum of all other termination events. We then wanted to gain insight into the contribution of termination for a distribution of radical chain lengths that have a defined deviation from i (i.e., $\pm\mu$) and centered at i. These results will determine whether radicals of chain lengths close to i contribute to most of the termination and therefore test the assumption that termination in RAFT-mediated polymerizations is between radicals of chain lengths similar to i. Figure 3 shows the ratio of $R_t^{i\pm\mu}/R_t$ as μ is varied from 0 to 50, where $R_t^{i\pm\mu}$ is calculated using eq 12.

$$R_t = \sum_{n=1}^{\infty}\sum_{m=1}^{\infty} k_t^{n,m}[P_n][P_m] \tag{11}$$

$$R_t^{i\pm\mu} = \sum_{n=i-\mu}^{i+\mu}\sum_{m=i-\mu}^{i+\mu} k_t^{n,m}[P_n][P_m] \tag{12}$$

At a deviation of ± 10 the graph shows that low values of both i and conversions are required to obtain a ratio of one. However, as the conversion is increased, the ratio decreased to below 0.1 at 80% conversion due to the broadening of the radical distribution with conversion (see Figure 2). The same trend is observed even if a broad radical distribution is considered (i.e., increasing the deviation of μ from 10 to 50). At low conversions the ratio of $R_t^{i\pm\mu}/R_t$ is close to one, but when μ was set equal to 50, the ratio decreased to close to 0.2 at 80% conversion. At first glance these results suggest that the RAFT-CLD-T method especially above the gel regime does not allow the accurate determination of $k_t^{i,i}(x)$, since the population of radicals with chain lengths close to i comprises a small contribution to the overall termination rate.

The accuracy of the RAFT-CLD-T method was therefore determined by calculating $\langle k_t^{i\pm\mu} \rangle$ for $\mu = 0$, 10, 20, 30, and 50 from eq 13 and using the radical distributions found by simulation.

$$\langle k_t^{i\pm\mu} \rangle = \frac{\sum_{n=i-\mu}^{i+\mu}\sum_{m=i-\mu}^{i+\mu} k_t^{n,m}[P_n][P_m]}{\left(\sum_{n=i-\mu}^{i+\mu}[P_n]\right)^2} \tag{13}$$

Figure 4 shows the $\langle k_t^{i\pm\mu} \rangle$ profiles as a function of conversion for the various values of μ. Curve a is the experimental data[15] determined using the RAFT-CLD-T method for the polymerization of MMA in the presence of CPDB (50 mM) and initiated with AIBN (10 mM). The simulations show that, regardless of the value of μ, all the $\langle k_t^{i\pm\mu} \rangle$ profiles fit the experimental data. Even when the whole radical distribution was used to calculate $\langle k_t \rangle$ (curve g), it gave good agreement between experiment (curve a) and the simulated $k_t^{i,i}(x)$ (curve b). The small deviation in curve g in the gel regime using the full radical distribution is most likely due to "short−long" termination at high conversion, leading to a slight overestimation of $k_t^{i,i}(x)$. (The contribution of "short−long" termination in RAFT-mediated polymerizations will be examined in the next section.) Therefore, the result of averaging the termination events generally leads to values of $\langle k_t \rangle$ being approximately equal to $k_t^{i,i}(x)$ up to high conversion. This significant result shows that the RAFT-CLD-T method can be used to obtain accurate $k_t^{i,i}$ values up to high conversions despite the strong chain length and conversion dependence in the gel regime. Further, these results support our k_t model developed previously[14] and therefore justify its use latter in this article.

"Short−Long" Termination in RAFT Polymerization. The theory of "short−long" termination has been implemented in kinetic models to describe conventional FRP[44−52] and is defined as termination between a "short" propagating radical (significantly less than the number-average chain length, i) and a "long" propagating radical close to i. This concept was formed on the basis that long polymeric radicals are slow to diffuse and therefore more likely to encounter and terminate with the faster diffusing "short" radicals, even though the long polymeric radicals are in much greater concentration. Figure 5 shows the ratio $R_t^{s,l}/R_t$, for the rate of "short−long" termination (eq 14) divided by the overall rate of termination up to the glass regime for the simulated RAFT-mediated polymerization of MMA at four different concentrations of AIBN (5, 10, 25, and 50 mM) in the presence of CPDB (50 mM). We define "short" chains of length below 5 and "long" chains as all chains greater than 5 units. This criterion was based on self-diffusion coefficients of PMMA oligomers obtained by Griffiths et al.,[53] in which oligomers greater than 5−6 monomer units fell onto a single diffusion curve. The rate of "short−long" termination, $R_t^{s,l}$, is defined as

$$R_t^{s,l} = \sum_{m=6}^{\infty}\sum_{n=1}^{5} k_t^{n,m}[P_n\cdot][P_m\cdot] \tag{14}$$

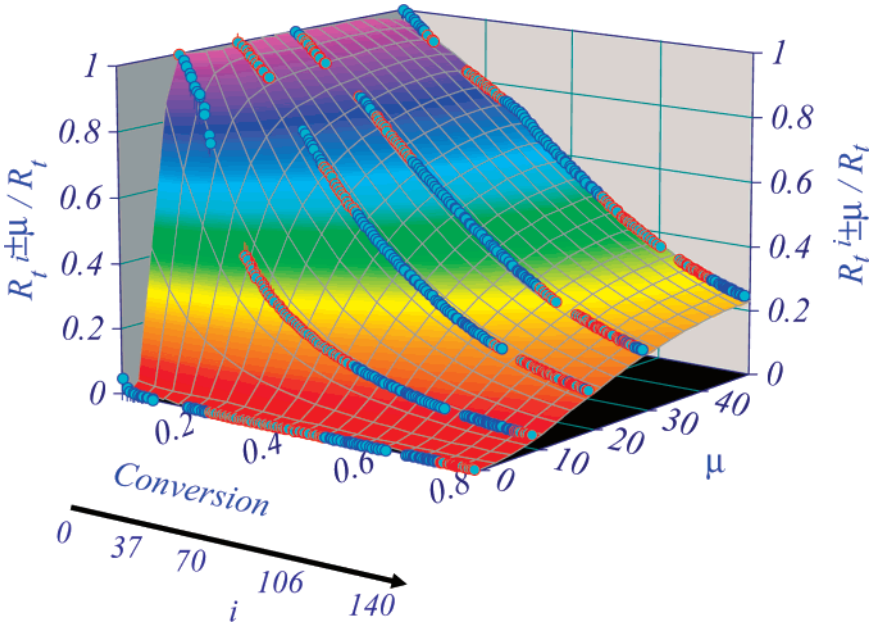

Figure 3. 3-Dimensional plots of simulated rates of termination in the living RAFT-mediated polymerization of methyl methacrylate (MMA, 9.34 M) using 50 mM RAFT agent and 10 mM azobis(isobutyronitrile) (AIBN) at 80 °C. Termination rates for radicals encompassed by an absolute deviation, $\pm\mu$, from the number-average chain length, i, divided by the total rate of termination, $R_t^{i\pm\mu}/R_t$ are given vs conversion (as well as i) and μ. Kinetic parameters: $C^0_{tr(pre)} = 15.2$,[14] $C^0_{tr(main)} = 140$,[61] $k_p = 1330$ L mol^{-1} s^{-1}, $f = 0.7$, and $k_d = 1 \times 10^{-4}$ s^{-1}. The evolution of i along the conversion axis is also shown.

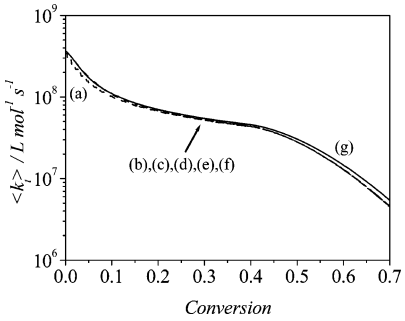

Figure 4. Average termination rate coefficient, $\langle k_t \rangle$, profiles for curve a experimental data from ref 15 for the RAFT-mediated bulk polymerization of methyl methacrylate (MMA, 9.34 M) in the presence of RAFT agent (CPDB, 50 mM) and initiated with azobis(isobutyronitrile) (AIBN, 10 mM) at 80 °C. Simulated $\langle k_t \rangle$ profiles for groups of radicals bounded by the absolute deviation, $\pm\mu$, from i, are given for (b) $\mu = 0$ (i.e., $k_t^{i,i}(x)$), (c) $\mu = 10$, (d) $\mu = 20$, (e) $\mu = 30$, and (f) $\mu = 50$. Curve g represents termination from the full radical distribution. Kinetic parameters: $C^0_{tr(pre)} = 15.2$,[14] $C^0_{tr(main)} = 140$,[61] $k_p = 1330$ L mol^{-1} s^{-1}, $f = 0.7$, and $k_d = 1 \times 10^{-4}$ s^{-1}.

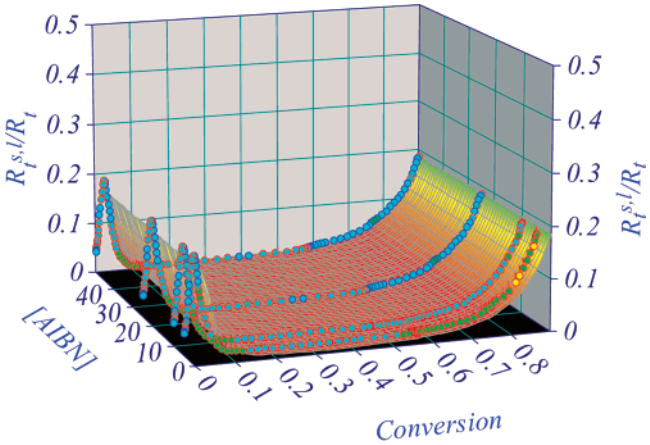

Figure 5. 3-Dimensional plot of simulated rates of "short−long" termination, $R_t^{s,l}$, divided by the overall rate of termination rate, R_t, as a function of both conversion and AIBN initiator concentration for the RAFT polymerization of methyl methacrylate (MMA, 9.34 M) in the presence of CPDB (50 mM) and initiated with azobis(isobutyronitrile) at 80 °C. "Short" is defined as chains equal to or less than 5 ($i \leq 5$) and "long" as chains greater than or equal to 6 ($i \geq 6$). The concentration of AIBN was varied from 5, 10, 25, and 50 mM. Kinetic parameters: $C^0_{tr(pre)} = 15.2$,[14] $C^0_{tr(main)} = 140$,[16] $k_p = 1330$ L mol^{-1} s^{-1}, $f = 0.7$, and $k_d = 1 \times 10^{-4}$ s^{-1}.

At conversions less than 10%, "short−long" termination accounts for ~20% of the termination rate, and between 10 and 50% conversion the ratio of $R_t^{s,l}/R_t$ was close to zero. Above 50% conversion (i.e., well into the gel regime), the ratio increased to 0.2 (at 80% conversion), suggesting "short−long" termination is the most likely cause for the deviation in curve g (Figure 4) at conversions above 50%. Interestingly, the increased AIBN concentration, even at the equivalent concentration to CPDB, did not influence the rate of "short−long" termination as would be intuitively expected, and thus for our system "short−long" termination can be neglected. Conversely, it is thought that in conventional FRP "short−long" termination is the dominant kinetic event, a point that will be examined in the latter part of the following section.

Model 2: Method of Moments. Simulations of RAFT Polymerization with Low Concentrations of CPDB. When modeling reactions for polymerizations with low concentrations of CPDB (e.g., 5, 10, and 20 mM) the full chain length distribution strategy (model 1) was computationally demanding due to the very large number of differential equations associated with high molecular weights. Model 2 utilizes the "method of moments" to determine the rate and number-average (M_n) and weight-average (M_w) molecular weights for RAFT polymerizations at low CPDB concentrations. In this approach, the composite k_t model and eq 9 were used to determine all values of $k_t^{i,j}$. Equation 10 was then solved for all values of $k_t^{i,j}$ using a Poisson distribution function for the radical distribution with the number-average chain length i at time t.

The comparison between experiment and simulations for three CPDB concentrations is given in Figure 6. The fit is excellent

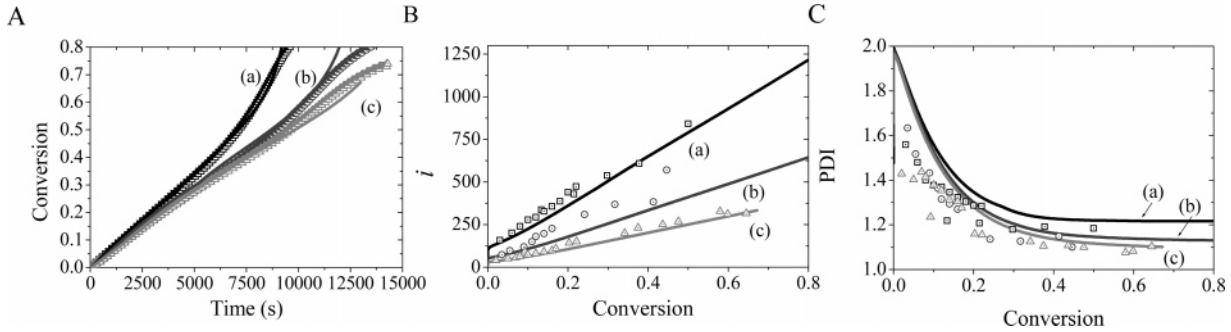

Figure 6. Kinetic plots for RAFT-mediated bulk polymerization of methyl methacrylate (MMA, 9.34 M) in the presence of RAFT agent (CPDB, 50 mM) and initiated with AIBN (10 mM) at 80 °C. Curves correspond to (a) [CPDB] = 4.98 mM and [AIBN] = 1.99 mM (□), (b) [CPDB] = 9.93 mM and [AIBN] = 2.01 mM (○), and (c) [CPDB] = 19.9 m and [AIBN] = 2.28 mM (Δ). Solid lines are simulated kinetic plots using the following kinetic parameters: $C^0_{tr(pre)} = 15.2$,[14] $C^0_{tr(main)} = 140$,[61] $k_p = 1330$ L mol^{-1} s^{-1}, $f = 0.7$, and $k_d = 1 \times 10^{-4}$ s^{-1}.

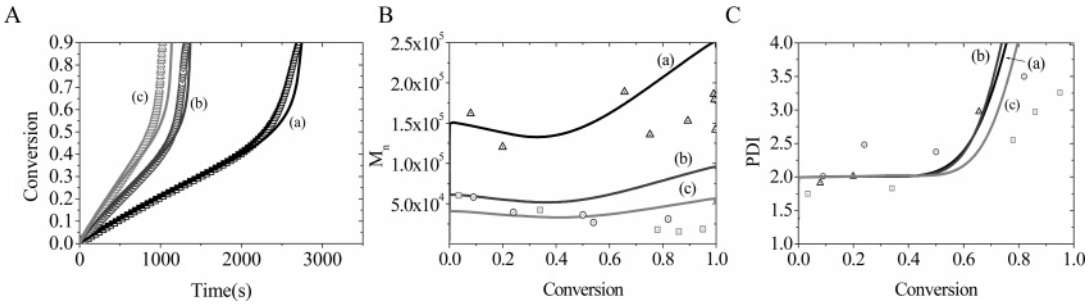

Figure 7. Kinetic plots for the conventional free radical polymerization of methyl methacrylate (MMA, 9.34 M) initiated with azobis(isobutyronitrile) (AIBN) at 80 °C. Curves correspond to (a) [AIBN] = 10 mM (Δ), (b) [AIBN] = 50 mM (○), and (c) [AIBN] = 100 mM (□). Solid lines are simulated kinetic plots by "method of moments" using the following kinetic parameters: $k_p = 1330$ L mol^{-1} s^{-1}, $f = 0.7$, and $k_d = 1 \times 10^{-4}$ s^{-1}.

for the three conversion profiles (Figure 6A) and shows that our modified "method of moments" incorporating a Poisson distribution is an acceptable strategy to simulate RAFT-mediated polymerizations for distributions with large chain lengths. The fit from dilute to gel regimes is pleasing and supports our model development and parameters. The fit with molecular weight data is also excellent (Figure 6B,C), providing additional support for this model strategy. However, the true test of our model strategy is to obtain agreement between simulation and experimental data from conventional free-radical polymerizations, which consists of distributions that are broad (PDIs > 2) and with a high proportion of long chains (>2000).

Simulations of Conventional Free Radical Polymerization Using Model 2. The same methodology as the RAFT-mediated polymerizations was used for conventional free-radical polymerizations, but a Schulz−Flory radical distribution function[34] was used instead to determine the radical distribution. Figure 7 shows the fit between experimental data and simulations at three concentrations of AIBN. The simulations provide an excellent fit to the conversion−time data and provide an excellent description of the transition from the dilute to gel regimes (i.e., the gradual transition found as the system reaches the gel onset conversion). The model slightly overestimates the time at onset of the gel effect in each experiment, which we attribute to approximating the radical chain length distribution using a Schulz−Flory distribution. The molecular weight data can also be fit with simulations (Figure 7B,C). Overall, these results are significant as they show that the $k_t^{i,i}(x)$ data determined via the RAFT-CLD-T method together with our composite k_t model and hybrid method of moments simulations can be easily utilized to predict conventional free-radical polymerizations. It is envisioned that the same modeling strategy used in this work will allow highly accurate predictions of rates and MWDs for other monomer systems.

"Short−Long" Termination in Conventional FRP. As discussed above, it has been thought that "short−long" termination in conventional FRP is a dominant process, especially in the gel regime. We denote "short" as chains that are less than 5 monomer units and "long" as all chains greater than 5 monomer units. Figure 8 shows the ratio $R_t^{s,l}/R_t$ up to a conversion of ∼80% for the conventional free-radical polymerization of MMA at three different concentrations of AIBN (10, 50, and 100 mM). At conversions below 10%, regardless of the AIBN concentration used, there is little or no contribution by "short−long" termination to the overall rate of termination. Above this conversion, $R_t^{s,l}/R_t$ increased linearly with conversion, approaching 0.8 (at ∼80% conversion), suggesting that even prior to the onset of the gel effect "short−long" termination is kinetically significant. In the gel regime, the rate of termination is dominated by "short−long" termination, in agreement with literature.[44−52]

Discussion on the Implications of "Short−Long" Termination. It has long been recognized that the radical chain length distribution (CLD) plays an important role in determining the kinetics of conventional free-radical polymerizations.[9] The modeling used in this work has shown that $k_t^{i,i}(x)$ determined from a narrow radical CLD (i.e., based on the RAFT-CLD-T method) can be used to describe termination in conventional free-radical polymerizations of broad radical CLDs. This is significant as it shows a direct relationship between the radical CLD, the extent of "short−long" termination, and the overall termination process. The ratio of "short−long" termination to the sum of all termination events found from simulated RAFT-mediated polymerizations (under "living" conditions), where the radical distribution is very narrow, shows that "short−long" termination is negligible, and termination occurs between radicals of similar chain length, *i*. Consequently, RAFT-mediated polymerization allows one to accurately examine the

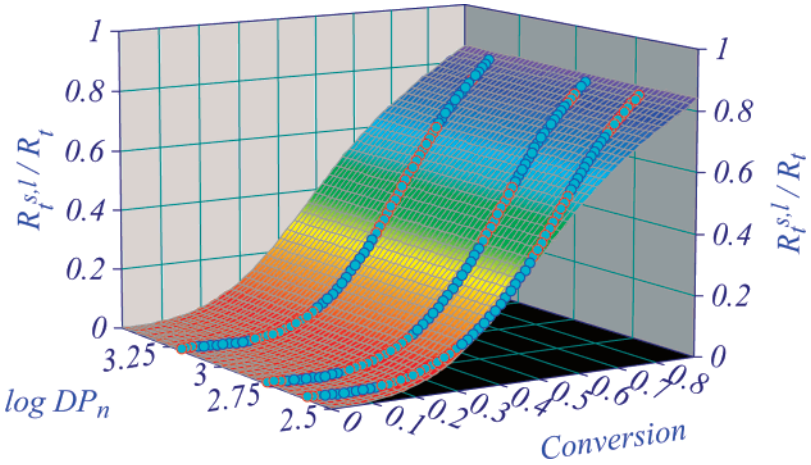

Figure 8. 3-Dimensional plot of calculated "short−long" termination rates, $R_t^{s,l}$, divided by the overall rate of termination rate, R_t, are given vs conversion and the degree of polymerization, DP_n, for the conventional free radical polymerization (FRP) of methyl methacrylate (MMA, 9.34 M) at 80 °C. "Short" equal $i \leq 5$ and "long" equal $i \geq 6$. Conditions: [AIBN] = 5, 10, and 50 mM. $R_t^{s,l}/R_t$ values were calculated for values of DP_n and conversion using the composite k_t model and a Schulz−Flory radical distribution function (see text). Kinetic parameters: $k_p = 1330$ L mol^{-1} s^{-1}, $f = 0.7$, and $k_d = 1 \times 10^{-4}$ s^{-1}.

specific effect of $i-i$ termination as a function of the conversion and average chain lengths, i, up to high conversion. This also allows one to examine the relationship between terminating polymeric radicals and the polymer matrix since both evolve together and are the same chain length. In conventional FRP where radical CLDs are broad, however, this is not the case. "Short−long" termination is significant and increases throughout the gel regime. This has important implications on the ability to examine the individual parameters affecting termination (such as chain length) and thus makes it difficult to discrimination between the various theories that have been proposed on the basis of physical mechanisms for termination.

It has been suggested that "short−long" termination may be a stand-alone explanation for the origin of the gel effect in FRP.[54,55] Our study shows that the gel effect can occur in the absence of "short−long" termination for living/controlled RAFT polymerizations. "Short−long" termination is, however, increasingly important above the gel effect in conventional FRP, in agreement with work presented elsewhere.[44,54] We therefore propose that "short−long" termination is an important consequence of the bimolecular termination process, particularly for broad radical CLDs, and has probably led to alternative theories like the free volume theory, which adequately describes the onset of the gel effect and reaction rate data at high conversions for conventional FRP.[55−57] However, in previous work using RAFT we found that the onset of the gel effect corresponded closely with the overlap of polymer coils (i.e., when the concentration reached a critical overlap concentration, c^*) for three very different polymers [poly(methyl methacrylate), poly(methyl acrylate), and poly(vinyl acetate)].[15] We believe that the absence of "short−long" termination in RAFT was the key to uncovering this physical relationship. This is probably the reason for the excellent agreement found in this work between our model and the experimental reaction rate and MWD data for both the RAFT polymerization and conventional FRP of MMA, for a wide range of molecular weight and conversion data. Given the correlation between the physical effects of chain overlap and the gel onset conversion, we expect similar physical phenomena to control termination in the gel and glass regimes. This is a focus of research currently being continued in our group.

Conclusion

In this work, we simulated RAFT-mediated and conventional free-radical polymerizations of MMA initiated with AIBN at 80 °C. The modeling strategy used comprised of a composite k_t model, developed in our previous work, and solving the differential equations for (i) all the chain lengths of all species (radical, dormant, and dead) or (ii) the various moments (i.e., "method of moments") and incorporating either a Poisson distribution for the RAFT-mediated polymerizations or a Schulz−Flory distribution for conventional FRPs. We found that our modeling strategy accurately predicted both rate of polymerization and evolution of the MWD in the RAFT polymerization of MMA under a range of experimental conditions. Examination of this simulation data showed that there was a negligible contribution of the rate of "$i-i$" termination compared to the overall rate of termination. However, and more importantly, analysis showed that $\langle k_t \rangle$ was approximately equal to $k_t^{i,i}$ even in the gel regime, thus validating the accuracy for the RAFT-CLD-T method to determine $k_t^{i,i}$ as a function of i and x even in the gel regime. Our modeling strategy was also used to simulate the rate of polymerization and MWD data for conventional free-radical polymerizations of MMA. "Short−long" termination was found to be a significant contributor to the termination process in these reactions, even prior to the onset of the gel effect. In contrast, "short−long" termination was absent from RAFT-mediated polymerizations and only gave a small contribution at very high conversions. This shows that RAFT-CLD-T method provides direct insight into the termination process of polymeric radicals of chain length close to i and their interactions with the polymer matrix up to high conversion. We envisage that the same composite modeling strategy used in this work can be easily applied to other monomers or free radical systems (i.e., ATRP, NMP, degenerative chain transfer, and conventional chain transfer polymerization) and thus allow highly accurate predictions of rates and MWDs.

Acknowledgment. G.J.-H. acknowledges financial support from the Australian Research Council (ARC), Australian Institute for Nuclear Science and Engineering (AINSE), and the University of Queensland (UQJRS scholarship). M.J.M.

acknowledges financial support from the ARC Discovery grant and receipt of a QEII Fellowship (ARC fellowship).

Supporting Information Available: Text giving the reaction scheme for reversible addition-fragmentation chain transfer (RAFT) living radical polymerization (LRP), differential equations written for the modeling program, derivations for eqs 6−8, and background on the use of the Schulz−Flory distribution function for modeling instantaneous chain length distributions. This material is available free of charge via the Internet at http://pubs.acs.org.

References and Notes

(1) Norrish, R. G. W.; Smith, R. R. *Nature (London)* **1942**, *150*, 336−337.
(2) Trommsdorf, E.; Kohle, H.; Lagally, P. *Makromol. Chem.* **1948**, *1*, 169−198.
(3) Matheson, M. S.; Auer, E. E.; Bevilacqua, E. B.; Hart, E. J. *J. Am. Chem. Soc.* **1949**, *71*, 497−504.
(4) Matheson, M. S.; Auer, E. E.; Bevilacqua, E. B.; Hart, E. J. *J. Am. Chem. Soc.* **1951**, *73*, 5395−5400.
(5) Benson, S. W.; North, A. M. *J. Am. Chem. Soc.* **1959**, *81*, 1339−1345.
(6) Benson, S. W.; North, A. M. *J. Am. Chem. Soc.* **1962**, *84*, 935−940.
(7) O'Driscoll, K.; Mahabadi, H. K. *J. Polym. Sci., Polym. Chem. Ed.* **1976**, *14*, 869−881.
(8) Allen, P. E. M.; Patrick, C. R. *Nature (London)* **1961**, *191*, 1194.
(9) Allen, P. E. M.; Patrick, C. R. *Makromol. Chem.* **1961**, *47*, 154−167.
(10) Olaj, O. F.; Kornherr, A.; Vana, P.; Zoder, M.; Zifferer, G. *Macromol. Symp.* **2002**, *182*, 15−30.
(11) Vana, P.; Davis, T. P.; Barner-Kowollik, C. *Macromol. Rapid Commun.* **2002**, *23*, 952−956.
(12) Buback, M.; Junkers, T.; Vana, P. *Macromol. Rapid Commun.* **2005**, *26*, 796−802.
(13) Barner-Kowollik, C.; Buback, M.; Egorov, M.; Fukuda, T.; Goto, A.; Olaj, O. F.; Russell, G. T.; Vana, P.; Yamazoe, H.; Zetterlund, P. B. *Prog. Polym. Sci.* **2005**, *30*, 605−643.
(14) Johnston-Hall, G.; Theis, A.; Monteiro, M. J.; Davis, T. P.; Stenzel, M. H.; Barner-Kowollik, C. *Macromol. Chem. Phys.* **2005**, *206*, 2047−2053.
(15) Johnston-Hall, G.; Stenzel, M. H.; Davis, T. P.; Barner-Kowollik, C.; Monteiro, M. J. *Macromolecules* **2007**, *40*, 2730−2736.
(16) Theis, A.; Davis, T. P.; Stenzel, M. H.; Barner-Kowollik, C. *Polymer* **2006**, *47*, 999−1010.
(17) Theis, A.; Feldermann, A.; Charton, N.; Stenzel, M. H.; Davis, T. P.; Barner-Kowollik, C. *Macromolecules* **2005**, *38*, 2595−2605.
(18) Theis, A.; Feldermann, A.; Charton, N.; Davis, T. P.; Stenzel, M. H.; Barner-Kowollik, C. *Polymer* **2005**, *46*, 6797−6809.
(19) Junkers, T.; Theis, A.; Buback, M.; Davis, T. P.; Stenzel, M. H.; Vana, P.; Barner-Kowollik, C. *Macromolecules* **2005**, *38*, 9497−9508.
(20) Theis, A.; Davis, T. P.; Stenzel, M. H.; Barner-Kowollik, C. *Macromolecules* **2005**, *38*, 10323−10327.
(21) Szwarc, M.; Levy, M.; Milkovich, R. *J. Am. Chem. Soc.* **1956**, *78*, 2656−2657.
(22) Szwarc, M. *Nature (London)* **1956**, *178*, 1168−1169.
(23) Mahabadi, H. K. *Macromolecules* **1985**, *18*, 1319−1330.
(24) Chiefari, J.; Chong, B. Y. K.; Ercole, F.; Krstina, J.; Jeffery, J.; Le, T. P. T.; Mayadunne, R. T. A.; Meijs, G. F.; Moad, C. L.; Moad, G.; Rizzardo, E.; Thang, S. H. *Macromolecules* **1998**, *31*, 5559−5562.
(25) (a) Monteiro, M. J. *J. Polym. Sci., Part A: Polym. Chem.* **2005**, *43*, 3189−3204. (b) Monteiro, M. J.; de Brouwer, H. *Macromolecules* **2001**, *34*, 349−352. (c) Plummer, R.; Goh, Y.-K.; Whittaker, A. K.; Monteiro, M. J. *Macromolecules* **2005**, *38*, 5352−5355.
(26) Johnston-Hall, G.; Monteiro, M. J. Tailoring Molecular Weight Distribution and Structure with Difunctional RAFT Agents. *ACS Symp. Ser.* **2006**, *944*, 421−437.
(27) Monteiro, M. J. *J. Polym. Sci., Part A: Polym. Chem.* **2005**, *43*, 5643−5651.
(28) Goh, Y.-K.; Monteiro, M. J. *Macromolecules* **2006**, *39*, 4966−4974.
(29) (a) Whittaker, M. R.; Monteiro, M. J. *Langmuir* **2006**, *22*, 9746−9752. (b) Whittaker, M. R.; Urbani, C. N.; Monteiro, M. J. *Langmuir* **2007**, *23*, 7887−7890.
(30) Whittaker, M. R.; Urbani, C. N.; Monteiro, M. J. *J. Am. Chem. Soc.* **2006**, *128*, 11360−11361.
(31) Malavasic, T.; Vizovisek, I.; Lapanje, S.; Moze, A. *Makromol. Chem.* **1973**, *175*, 873−880.
(32) Barner-Kowollik, C.; Buback, M.; Charleux, B.; Coote, M. L.; Drache, M.; Fukuda, T.; Goto, A.; Klumpermann, B.; Lowe, A. B.; Mcleary, J. B.; Moad, G.; Monteiro, M. J.; Sanderson, R. D.; Tonge, M. P.; Vana, P. *J. Polym. Sci., Part A: Polym. Chem.* **2006**, *44*, 5809−5831.
(33) Bamford, C. H.; Tompa, H. *Trans. Faraday Soc.* **1954**, *50*, 1097−1115.
(34) Flory, P. J. *Principles of Polymer Chemistry;* Cornell University Press: Ithaca, NY, 1953.
(35) Russell, G. T. *Macromol. Theory Simul.* **1994**, *3*, 439−468.
(36) Russell, G. T. *Aust. J. Chem.* **2002**, *55*, 399−414.
(37) Moad, G.; Solomon, D. H. *The Chemistry of Free Radical Polymerization*, 1st ed.; Pergamon: Oxford, 1995.
(38) Heuts, J. P. A.; Gilbert, R. G.; Radom, L. *Macromolecules* **1995**, *28*, 8771−8781.
(39) Gridnev, A. A.; Ittell, S. D. *Macromolecules* **1996**, *29*, 5864−5874.
(40) Olaj, O. F.; Vana, P.; Zoder, M.; Kornherr, A.; Zifferer, G. *Macromol. Rapid Commun.* **2000**, *21*, 913−920.
(41) Olaj, O. F.; Kornherr, A.; Zifferer, G. *Macromol. Theory. Simul.* **1998**, *7*, 501−508.
(42) Olaj, O. F.; Zifferer, G.; Gleixner, G. *Makromol. Chem., Rapid Commun.* **1985**, *6*, 773−784.
(43) Olaj, O. F.; Zifferer, G.; Gleixner, G. *Macromolecules* **1987**, *20*, 839−850.
(44) O'Shaughnessy, B.; Yu, J. *Macromolecules* **1994**, *27*, 5067−5078.
(45) O'Shaughnessy, B.; Yu, J. *Macromolecules* **1998**, *31*, 5240−5254.
(46) O'Shaughnessy, B.; Yu, J. *Phys. Chem. B* **1994**, *73*, 1723−1726.
(47) O'Shaughnessy, B.; Yu, J. *Macromolecules* **1994**, *27*, 5079−5085.
(48) Friedman, B.; O'Shaughnessy, B. *Macromolecules* **1993**, *26*, 5726−5739.
(49) Russell, G. T.; Gilbert, R. G.; Napper, D. H. *Macromolecules* **1992**, *25*, 2459−2469.
(50) Buback, M.; Gilbert, R. G.; Hutchinson, R. A.; Klumpermann, B.; Kutcha, F.-D.; Manders, B. G.; O'Driscoll, K.; Russell, G. T.; Schweer, J. *Macromol. Chem. Phys.* **1995**, *196*, 3267−3280.
(51) Scheren, P. A. C.; Russell, G. T.; Sangster, D. F.; Gilbert, R. G.; German, A. L. *Macromolecules* **1995**, *28*, 3637−3648.
(52) Russell, G. T. *Macromol. Theory. Simul.* **1995**, *4*, 497−517.
(53) Griffiths, M. C.; Strauch, J.; Monteiro, M. J.; Gilbert, R. G. *Macromolecules* **1998**, *31*, 7835−7844.
(54) Russell, G. T.; Gilbert, R. G.; Napper, D. H. *26* **1993**, *14*, 3538−3552.
(55) O'Neil, G. A.; Wisnudel, M. B.; Torkelson, J. M. *Macromolecules* **1996**, *29*, 7477−7490.
(56) Balke, S. T.; Hamielec, A. E. *J. Appl. Polym. Sci.* **1973**, *17*, 905−949.
(57) O'Neil, G. A.; Wisnudel, M. B.; Torkelson, J. M. *Macromolecules* **1998**, *31*, 4537−4545.
(58) Beuermann, S.; Buback, M.; Davis, T. P.; Gilbert, R. G.; Hutchison, R. A.; Friedrich, O. O.; Russell, G. T.; Heuts, J. P. A.; van Herk, A. M. *Macromol. Chem. Phys.* **2003**, *198*, 1545−1560.
(59) Bevington, J. C.; Melville, H. W.; Taylor, R. P. *J. Polym. Sci.* **1954**, *14*, 463−476.
(60) Brandup, J.; Immergut, E. H.; Grulke, E. A. *Polymer Handbook;* J. Wiley & Sons: New York, 1989.
(61) Goto, A.; Sato, K.; Tsujii, Y.; Fukuda, T.; Moad, G.; Rizzardo, E.; Thang, S. H. *Macromolecules* **2001**, *34*, 402−408.
(62) Achilias, D. S.; Kiparissides, C. *Macromolecules* **1992**, *25*, 3739−3750.

MA070984D